NASA Technical Paper 1662

A Numerical Technique for Calculation of the Noise of High-Speed Propellers With Advanced Blade Geometry

Paul A. Nystrom and F. Farassat

JULY 1980

NASA Technical Paper 1662

A Numerical Technique for Calculation of the Noise of High-Speed Propellers With Advanced Blade Geometry

Paul A. Nystrom and F. Farassat
Langley Research Center
Hampton, Virginia

National Aeronautics
and Space Administration

**Scientific and Technical
Information Office**

1980

SUMMARY

This paper discusses a numerical technique and a computer program developed for the prediction of the noise of propellers with advanced geometry. The blade upper and lower surfaces are described by a curvilinear coordinate system, which is also used to divide the blade surfaces into panels. Two different acoustic formulations in the time domain are used to improve the speed and efficiency of the noise calculations: an acoustic formulation with the Doppler factor singularity for panels moving at subsonic speeds and the collapsing sphere formulation for panels moving at transonic or supersonic speeds. This second formulation involves a sphere which is centered at the observer position and whose radius decreases at the speed of sound. The acoustic equation consists of integrals over the curve of intersection for both the sphere and the panels on the blade. Algorithms used in some parts of the computer program are discussed briefly. Some comparisons with measured acoustic data for two model high-speed propellers with advanced geometry are also presented.

INTRODUCTION

Man has used propellers since the early days of flight. In recent years, however, other propulsion systems such as turbofans have replaced propellers on large commercial and military aircraft. Many factors, such as cruising speed limitation, propulsion system weight, noise, and operating cost of propeller-driven aircraft, have led to their replacement. More recently, the energy crisis has created a new incentive to look at propellers for use in future aircraft.

It is well-known that the efficiency of propellers is generally higher than that of jet-driven propulsors. However, a conventional propeller for an aircraft flying at Mach 0.8, which is the speed of current subsonic airliners, may generate an excessive amount of noise. The problem of noise alone is sufficient to make conventional propellers unattractive for consideration in future airliners. If propellers are to be used in large transports, an advanced geometry to reduce noise must be considered. Such a step has been taken in recent years, and model tests have shown the effectiveness of advanced designs both in reducing the noise and maintaining high efficiency.

Since both model and full-scale tests of propellers are very expensive and time consuming, considerable effort has been made to predict the noise theoretically to complement the aerodynamic calculations. Advances in the field of the aeroacoustics of rotating blades have helped in the understanding of the basic noise generation mechanisms of propellers with advanced geometry. This paper discusses one of the noise prediction methods developed specifically for these propellers. First, the formulations, based on linear acoustics, used to calculate the noise are presented. The computing algorithm and a discussion of the details of some of the subroutines are presented next. Finally, some examples

for which test results are available are given to point out the capabilities and the weaknesses of the prediction method. On the whole, the method provides a versatile and useful tool for predicting the noise of both conventional and advanced propellers.

SYMBOLS AND ABBREVIATIONS

b	local chord
c	speed of sound in undisturbed medium
C_p	pressure coefficient
d	distance of observer from x_3-axis
$f(\vec{x},t) = 0$	equation of blade surface
$g = \tau - t + \frac{r}{c} = 0$	equation of collapsing sphere centered at observer position $\vec{x}$
i,j	indices of summation
l_i	local force (per unit area) on fluid in direction i
$K(\tau)$	function defined by equation (12)
L.E.	leading edge
M	Mach number
M_r	Mach number in radiation direction
$\vec{n}$	unit normal vector to surface $f = 0$
$p'(\vec{x},t)$	acoustic pressure
PCA	pitch change axis
Q	fraction of chord as measured from leading edge
R	radius
$\vec{r}$	radiation vector, $\vec{x} - \vec{y}$
r	length of radiation vector, $\lvert\vec{x} - \vec{y}\rvert$
$\hat{\vec{r}}$	unit radiation vector

S	surface area of blade
t	observer time
T.E.	trailing edge
v_n	local normal velocity of blade surface
$\vec{v}$	local velocity of blade surface
$\vec{x}$	observer position fixed with respect to undisturbed medium
$\vec{x}_f$	observer position in fixed frame
$\vec{x}_m$	observer position in moving frame
$\vec{y}$	source position
OASPL	overall sound pressure level, dB (re 20 μPa)
SPL	sound pressure level, dB (re 20 μPa)
α	blade pitch angle
β	azimuthal coordinate of observer
Γ	curve of intersection of blade surface and collapsing sphere
$\delta(f)$	Dirac delta function
$\vec{\eta}$	rotating frame coordinates; η is radius in polar coordinates
θ	angle between surface normal and radiation vector
π	= 3.141592654
ρ_o	density of undisturbed medium
τ	source time
τ^*	emission time
ϕ	azimuthal coordinate of source at time $\tau > 0$
ψ	azimuthal coordinate of source at $\tau = 0$
ω	rotational speed of blades

Subscripts:

f	frame fixed with respect to undisturbed medium
r	radiation direction
ref	reference
ret	evaluated at $\tau = \tau^*$
o	conditions of undisturbed medium
1,2,3	coordinate directions

Vectors are denoted by $\rightarrow$; symbols alone represent magnitude of the vector.

THEORETICAL FORMULATION

Propeller noise generation and prediction have been studied for almost 60 years (ref. 1). Sufficient advances have been made during this period so that reliable noise prediction can be made in many cases. Almost all the prediction methods available today rely on linear acoustics. Theoretically, the problem of noise prediction can be reduced to the solution of the wave equation with a given distribution of sources on a moving boundary (propeller blade surface). There are basically two steps in the prediction problem:

1. The determination of the source distribution on the moving boundary

2. Solving the three-dimensional wave equation with the specified source distributions on the blade surface

There have been many successful prediction theories in the past such as those by Gutin (ref. 2), Deming (ref. 3), Garrick and Watkins (ref. 4), and Lowson (ref. 5). However, all these theories have some limitations which make them unsuitable for applications to propellers with advanced geometry. Some of these limitations are the assumptions of compactness of the acoustic sources and far-field position of the observer. Two unusual features of advanced propellers which must be considered in the development of a prediction technique are

1. The blades have considerable twist and out-of-plane sweep. Therefore, sources on the blade surface should not be approximated by sources in the plane of the propeller.

2. The propeller helical tip speed is supersonic. The formulations used in calculating the noise must be capable of handling supersonic sources.

These two features of advanced propellers and some other requirements, such as the need for near-field calculations, led to the selection of a purely numer-

ical approach for noise calculations. The formulations used are two forms of the solution of the Ffowcs Williams and Hawkings (FW-H) wave equation (ref. 6), where the quadrupole term has been dropped. Thus, only the surface source terms have been retained. The effect of neglecting the quadrupole term in the FW-H equation will be discussed later.

The governing equation for the determination of the acoustic pressure $p'(\vec{x},t)$ is

$$\frac{1}{c^2}\frac{\partial^2 p'}{\partial t^2} - \nabla^2 p' = \frac{\partial}{\partial t}\left[\rho_o v_n |\nabla f|\ \delta(f)\right] - \frac{\partial}{\partial x_i}\left[l_i |\nabla f|\ \delta(f)\right] \tag{1}$$

where c and ρ_o are the speed of sound and the density in the undisturbed medium, respectively, and v_n is the local normal velocity on the blade surface, which is described by the equation $f(\vec{x},t) = 0$. The local force (per unit area) on the fluid by the blade surface is denoted by l_i, and $\delta(f)$ is the Dirac delta function. Equation (1) is known as the FW-H equation (ref. 6).

The two forms of solution for equation (1) which were derived in reference 7 and used to calculate propeller noise are

$$4\pi p'(\vec{x},t) = \frac{1}{c}\frac{\partial}{\partial t}\int_{f=0}\left[\frac{\rho_o c v_n + l_r}{r|1 - M_r|}\right]_{ret} dS$$

$$+ \int_{f=0}\left[\frac{l_r}{r^2|1 - M_r|}\right]_{ret} dS \tag{2}$$

$$4\pi p'(\vec{x},t) = \frac{\partial}{\partial t}\int_{\substack{f=0\\g=0}}\frac{\rho_o c v_n + l_r}{r \sin\theta}\, d\Gamma\, d\tau + \int_{\substack{f=0\\g=0}}\frac{c l_r}{r^2 \sin\theta}\, d\Gamma\, d\tau \tag{3}$$

In equations (2) and (3), dS is an element of surface area on the blade $f = 0$, and $d\Gamma$ is an element of length of the curve of intersection for the surfaces $f = 0$ and $g = \tau - t + (r/c) = 0$. The symbol θ represents the angle between the normal to the surface $f = 0$ and the radiation vector $\vec{r} = \vec{x} - \vec{y}$. In equation (2), $M_r = \vec{v} \cdot \hat{\vec{r}}/c$, where $\vec{v}$ is the local velocity on

the blade surface and $\hat{\vec{r}} = \vec{r}/r$, the unit vector in the radiation direction. The collapsing sphere method discussed in this paper refers to application of equation (3) (see ref. 7).

To apply the above equations, the right sides of both equations are written in finite difference forms. Each blade is divided into small panels, and depending on whether M_r is less than or greater than 0.98, equation (2) or equation (3), respectively, is used. The observer time differentiation is also done numerically.

The computer program discussed in this paper can handle cases in which the observer has the same forward speed as the propeller. This is achieved by letting $\vec{x}_m$ be the position of the observer in the moving frame; then the observer position in the frame fixed to the undisturbed medium is

$$\vec{x}_f = \vec{x}_m + \int_0^t \vec{v}(t')\, dt'$$

where $\vec{v}(t')$ is the forward velocity of the propeller. Therefore, in the moving frame, the numerical value of $p'(\vec{x}_m, t)$ is the same as $p'(\vec{x}_f, t)$. In this case, $\vec{x}_f = \vec{x}_f(\vec{x}_m, t)$, and this is known if the motion of the propeller is specified.

THE NUMERICAL APPROACH TO NOISE CALCULATIONS

In this section the method of implementing equations (2) and (3) on a computer for propeller noise calculations is presented. Each blade is first divided into panels in a manner discussed in the next subsection. The contribution of ith panel to the acoustic pressure, denoted by p_i', from equations (2) and (3), may be written as

$$4\pi p_i'(\vec{x},t) = \frac{1}{c}\frac{\Delta}{\Delta t}\left[\left(\frac{\rho_o c v_n + l_r}{r|1 - M_r|}\right)_i\right]_{ret} \Delta S_i + \left[\left(\frac{l_r}{r^2|1 - M_r|}\right)_i\right]_{ret} \Delta S_i \qquad (4)$$

$$4\pi p_i'(\vec{x},t) = \frac{\Delta}{\Delta t}\sum_j \left(\frac{\rho_o c v_n + l_r}{r \sin\theta}\right)_i \Delta\Gamma(\tau_j)\, \Delta\tau + \sum_j \left(\frac{c l_r}{r^2 \sin\theta}\right)_i \Delta\Gamma(\tau_j)\, \Delta\tau \qquad (5)$$

The contributions of all the panels are added together to obtain the acoustic pressure signature $p'(\vec{x},t)$. The numerical differentiations in equations (4) and (5) are performed after the summations on all panels are performed.

Although the concept behind the application of these equations is simple, considerable care must be exercised in selection of an algorithm for computer programming for several reasons. First, past experience has indicated that acoustic calculations based on the above equations are sensitive to errors. Both the specification of blade geometry and the emission time calculation must be done as precisely as possible. Second, since noncompact source calculations are generally time consuming, the speed of execution for subroutine algorithms becomes an important consideration.

Figure 1 shows the flow chart for the computer code developed at Langley Research Center. Each blade is divided into panels in a manner that is discussed in the next section. The observer position and time are prescribed next. Depending on the value of the helical tip Mach number of each panel center, one of the two schemes for the calculation of the emission time is used. Once the emission time (or times) of a panel is known, the value of M_r, the relative Mach number in the observer direction, is calculated. If this M_r is less than a prescribed value (usually taken here as 0.98), then equation (4) is used for that panel. Otherwise, equation (5) is used. Therefore, for a given observer position and time, equation (4) is used for some panels on the blade surface, and equation (5) is used for the remaining panels to obtain the acoustic pressure $p'(\vec{x},t)$. The combination of the two formulas improves the speed and efficiency of the acoustic calculations. In general, the implementation of equation (4) on a computer is simpler and faster than that of equation (5). On the other hand, equation (4) cannot be used when M_r is close to 1, and thus equation (5) must be used.

In the following subsections, further details of important parts of the computer program are presented.

Blade Coordinate Frame and Subdivision

The blades of advanced propellers can have substantial amounts of twist and sweep. Thus, blade sources should not be assumed to be in a plane. For this reason, a coordinate frame as shown in figure 2 is used to account for the three-dimensional character of the blades. This frame, called the $\vec{\eta}$-frame, is fixed to each blade. The center of this frame is on the propeller axis, and the η_2-axis coincides with the pitch change axis (PCA) of the propeller.

To describe the blade, the leading-edge curve of the blade is given as a function of distance along the pitch change axis η_2. Then the chord, airfoil section, twist, and thickness ratio of the blade are specified as functions of η_2. The specification of these parameters is sufficient to describe the blade completely.

To subdivide the blades into panels, each blade is cut in the radial direction by planes perpendicular to the pitch change axis. In the chordwise direction, a new nondimensional variable Q is introduced. This variable is the distance from the leading edge along the local chord divided by the local chord b. The upper and lower surfaces of the blade are now mathematically described as functions of the variables η_2 and Q. Figure 2 shows this curvilinear coordinate system for blade description.

The blade is subdivided into panels by specifying the number of spanwise and chordwise divisions. This division gives the increments $\Delta\eta_2$ and ΔQ for each panel. If $\vec{\eta}$ is the position vector of a point on the blade surface, the surface area of the panel is approximated by the following relation:

$$\Delta S = \left| \frac{\partial \vec{\eta}}{\partial \eta_2} \times \frac{\partial \vec{\eta}}{\partial Q} \right| \Delta\eta_2 \, \Delta Q \tag{6}$$

The unit normal to the blade surface as used in the acoustic calculations is given by

$$\vec{n} = \frac{\left(\frac{\partial \vec{\eta}}{\partial \eta_2} \times \frac{\partial \vec{\eta}}{\partial Q} \right)}{\left| \frac{\partial \vec{\eta}}{\partial \eta_2} \times \frac{\partial \vec{\eta}}{\partial Q} \right|} \tag{7}$$

For thickness noise calculations, the upper and lower blade surfaces were divided into panels. For loading noise calculations, the mean surface comprised of local chord lines is divided into panels. Different blade subdivisions were used for calculation of loading noise because details of the surface pressure distributions are not generally available.

Calculation of the Emission Time

If the source and the observer times are τ and t, respectively, and the distance between the observer and the source is r, the emission time $\tau = \tau^*$ is calculated from the relation

$$c(\tau^* - t) + r = 0 \tag{8}$$

The emission time is the time when the sources on the panel emit sound which arrives at the observer at the time t. The source position $\vec{y}$ is a function of τ, so that r itself is a function of τ. Because of the trigonometric terms in r (see eq. (11)), equation (8) cannot be solved for τ^* in closed form. A numerical method must be used. Two schemes are used depending on the speed of the source.

Scheme 1.- When the observer time and position are fixed, one can show that for a given source in motion

$$\frac{\partial g}{\partial \tau} = 1 - M_r \tag{9}$$

where $g = \tau - t + (r/c)$. Equation (8) demonstrates that, viewed as a function of a single variable τ, the emission times of a source in motion are the zeros of function g. For sources in subsonic motion, one has $M_r < 1$ and therefore $\frac{\partial g}{\partial \tau} > 0$. This means that the function g is a strictly increasing function of τ and thus can have only one zero.

These facts suggested the use of Newton's method to develop a fast iterative scheme to find the emission times of each panel on the blade. This scheme is used for panels with helical Mach numbers below 0.95. To speed up the convergence of iteration, the known emission time of a nearby panel is used as the initial guess for the emission time of the next panel. The use of this scheme in the program has resulted in shortened computation time for general aviation propellers which operate at subsonic tip speeds.

Scheme 2.- This scheme is used when the helical Mach number of a panel is above 0.95. One may get multiple emission times for panels moving at supersonic speeds. Because of this fact, scheme 1 will not work without narrowing down the range of search for each root of equation (8). This new method is called scheme 2 and is discussed briefly in the following paragraphs.

Assume that the source lies in the x_1x_2-plane at source time $\tau = 0$. The source position at this time is described by (η,ψ) in polar coordinates as shown in figure 3. The source rotates around the x_3-axis (propeller axis) at an angular velocity of ω and moves forward in the positive direction of this axis at velocity v_3. The $\vec{x}$-frame is fixed to the undisturbed medium and is not in motion. The observer position and time are $\vec{x}$ and t, respectively. Viewed by the observer in this frame, the source path is a helix. From equation (8), the following equation may be obtained:

$$c^2(\tau - t)^2 - r^2 = 0 \tag{10}$$

With only the solutions $\tau \leq t$ being physically acceptable. The square of the distance between the source and the observer can be written as follows:

$$r^2 = x_3^2 + d^2 + \eta^2 - 2\, d\eta \cos(\phi - \beta) + v_3^2\tau^2 - 2x_3v_3\tau \tag{11}$$

where $\phi = \psi + \omega\tau$, and d is the distance of the observer from the x_3-axis (see fig. 3). The angle β is shown in figure 3. Assuming $v_3/c = M < 1$ and $\tau_o = x_3/c$, equation (10) can now be written as

$$K(\tau) \equiv c^2(1 - M^2)\tau^2 - 2c^2(t - M\tau_o)\tau + c^2(t^2 - \tau_o{}^2)$$

$$= d^2 + \eta^2 - 2\, d\eta \cos(\phi - \beta) \qquad (12)$$

The graphs of

$$K(\tau) = c^2(1 - M^2)\tau^2 - 2c^2(t - M\tau_o) + c^2(t^2 - \tau_o{}^2)$$

$$K(\tau) = d^2 + \eta^2 - 2\, d\eta \cos(\phi - \beta)$$

are a parabola and a sinusoidal curve in the τK-plane, respectively. Thus, to find the roots of equation (12), the points of intersection of a parabola and a sinusoidal curve must be determined. These roots must lie between the points of intersection of the lines $K = (d \pm \eta)^2$ parallel to the τ-axis in the τK-plane. These lines are obtained by setting $\cos(\phi - \beta)$ in equation (12) equal to -1 and 1, respectively.

Not all the roots of equation (12) are emission times because the requirement $\tau \leqq t$ is not satisfied for all the roots. Only the roots obtained by the intersection of the parabola and the sinusoidal curve which are to the left of the axis of the parabola are the emission times. One can graphically demonstrate that only an odd number of emission times are obtained if multiple roots are counted by their multiplicity (e.g., two equal roots are counted as two roots). The method of modified regula falsi discussed in reference 8 is used to find the roots of equation (12). In the implementation of this method, the intervals in which each root of the equation lie are found first. An iterative method is then used in each interval to find the roots. This method is more time consuming to implement on the computer than that of scheme 1. However, of the several methods for finding emission time tried in the course of the development of the computer program, the scheme based on modified regula falsi was the most satisfactory, both in precision and speed and in guaranteeing that all the roots would be found.

Application of the Collapsing Sphere Technique

The collapsing sphere technique based on equation (3) or equation (5) is time consuming on the computer and should be used for as few panels as possible. Therefore, this method was used for a panel only if the Mach number in the radiation direction at any of the emission times was greater than a prescribed value (usually taken as 0.98). To calculate the length $\Delta\Gamma$ of the curve of the intersection of the collapsing sphere and a panel, the edges of the panel were assumed to be straight lines. The points of intersection were calculated analytically. At least 10 intersections of the collapsing sphere with each panel were used in equation (5) when this method was employed. Only intersections with the mean surface of the blade formed by the chord lines, rather than the upper and lower surfaces, were taken to save computing time.

APPLICATIONS OF THE NUMERICAL TECHNIQUE

The present numerical technique has been used successfully for both conventional and advanced propellers. Some acoustic calculations and comparisons with experimental measurements for a conventional propeller were published in the paper by Mixson et al. (ref. 9). In the present paper, the results of a series of model tests of advanced propellers are presented. These tests were conducted in the Acoustic Research Tunnel, an anechoic wind tunnel, of United Technologies Research Center (ref. 10).

The model propellers were operated inside an air jet. The microphones were located outside the shear layer of this jet. For this reason, corrections had to be made for both the measured levels of the acoustic spectra and the microphone positions. These corrections, which were based on Amiet's theory (ref. 11), were supplied by the manufacturer. In this paper, the corrected microphone positions and the measured acoustic data are reported.

Acoustic calculations for two blade designs, SR-1 and SR-3, are presented here. The SR-1 blade was the first design created for studying the effect of planform sweep on the generation of noise. Figure 4 shows the planform of this blade design. The SR-3 design, also shown in figure 4, was acoustically optimized to reduce the peak level of the acoustic spectrum at the design condition. This optimization has had a favorable effect in reducing noise in all directions.

Table 1 summarizes the operating conditions and some related propeller data for the two blade designs. Table 2 presents the microphone positions. The numbering of microphone positions used in reference 10 has been retained to reduce confusion. Figures 5 and 6 present the blade form curves and the radial distribution of lift coefficient for the two blade designs, respectively. These data were supplied by the manufacturer. In the acoustic calculations, the chordwise pressure distribution on the blades was assumed to be parabolic. This assumption was necessary because of a lack of theoretical and experimental data for the range of Mach numbers of interest. Because of the three-dimensionality of the flow, particularly near the tip of the blades, the validity of the application of strip theory to obtain the chordwise pressure distribution is questionable. The chordwise pressure distribution has an effect on the level of the acoustic spectrum. This effect can influence the shape of the acoustic spectrum, particularly for advanced high-speed propellers (ref. 12).

Figures 7 to 11 present the theoretical and measured acoustic pressure signatures and spectra for the SR-1 blade at five microphone positions. Figures 12 to 14 present similar results for the SR-3 blade design at three microphone positions. Symbols on the waveforms mark the position of peak values. These results are typical of a number of high-speed propeller calculations performed using the present program. In all these calculations, the blade subdivision was as follows. In the spanwise direction, 20 coarse divisions were selected in such a way that the smaller $\Delta\eta_2$ resulted near the blade tip. In the chordwise direction, 5 divisions in the first 5 percent of the chord and 10 divisions in the remainder of the chord were selected to define the coarse mesh sizes. For

panels traveling above a helical Mach number of 0.98, each panel was divided further into three spanwise divisions and two chordwise divisions. These divisions constituted the fine mesh sizes.

The most striking feature of all these calculations is that the theoretical waveforms reproduce the basic characteristics of the measured waveforms. Even some of the details of the measured waveforms, such as the narrow and broad peaks in the acoustic pressure signatures, also appear in the calculated signatures.

The theoretical calculations differ from the measured data in two respects. First, the level of the lower harmonics of the acoustic spectra are generally underestimated, particularly for those near the first peak of the spectra. Second, the width of the main pulse of the acoustic pressure signature is underestimated or, equivalently, the first dip in the theoretical spectrum is located at a higher harmonic number than that for the measured spectrum. Both these discrepancies between the measured and calculated results are attributed to the neglect of nonlinearities. Much effort has been spent recently to include the effect of nonlinearities to improve linear calculations (refs. 13 and 14). These methods, which are basically numerical in nature, have not yet fully explained the discrepancies between the measured and the calculated (linear acoustic) results. However, they have served to strengthen the belief that linear acoustic calculations must be supplemented or corrected in order to explain measured data for high-speed rotating blades.

The theoretical acoustic calculations for the SR-3 blade generally agree better with measured data than those for the SR-1 blade. The reason is believed to be the reduction of quadrupole noise from the transonic flow region around the SR-3 blade (ref. 15). The calculations reported here agree well with those reported by Hanson (ref. 12).

For calculations based on the SR-3 blade design (figs. 13 and 14), the high frequency oscillations of the theoretical waveforms are attributable to weak Prandtl-Meyer waves from the blade surfaces. These waves are generated because the blades are approximated by panels which at their boundary make a small, but finite, angle to each other. The waves are radiated from the corners where the edges of two panels meet. These oscillations are more obvious for SR-3 blades, since their helical tip Mach number is higher than that for SR-1 blades. The overestimation of levels of high harmonics of the spectra for SR-3 blades is the manifestation of the same phenomenon in the frequency domain. The strongest waves originate from the leading and the trailing edges of the blade. The oscillations observed in the calculated waveforms are most likely induced by the leading and trailing edges of blade strips located at different distances from the blade center. This phenomenon will always appear as long as linear acoustic theory is used with a finite number of panels on the blades for noise calculations. An acceptable but artificial method of removing these high frequency oscillations is numerical filtering of the theoretical data.

CONCLUDING REMARKS

This paper discusses a method for calculating the noise of advanced propellers. A computer program based on this method is coded so that high-speed propellers with advanced blades can be easily handled. The propeller may be assumed to be in forward flight with the observer stationary with respect to the medium or in motion with forward speed of the propeller. Comparison of theoretical and measured acoustic data for propellers in forward motion has shown satisfactory agreement for conventional propellers. However, for high-speed propellers, both the levels of some harmonics (usually near the first peak) and the width of the main pulse of the pressure signature are somewhat underestimated. These discrepancies between theoretical and measured data are caused by flow nonlinearities not included in the program discussed here. This program provides a useful and versatile tool for predicting the noise of propellers at the design stage, particularly for studying the relative noise levels between several propeller designs.

Langley Research Center
National Aeronautics and Space Administration
Hampton, VA 23665
April 21, 1980

REFERENCES

1. Morfey, C. L.: Rotating Blades and Aerodynamic Sound. J. Sound & Vib., vol. 28, no. 3, June 8, 1973, pp. 587-617.

2. Gutin, L.: On the Sound Field of a Rotating Propeller. NACA TM 1195, 1948.

3. Deming, A. F.: Noise From Propellers With Symmetrical Sections at Zero Blade Angle, II. NACA TN 679, 1938.

4. Garrick, I. E.; and Watkins, Charles E.: A Theoretical Study of the Effect of Forward Speed on the Free-Space Sound-Pressure Field Around Propellers. NACA Rep. 1198, 1954. (Supersedes NACA TN 3018.)

5. Lowson, M. V.: The Sound Field for Singularities in Motion. Proc. R. Soc. (London), ser. A, vol. 286, no. 1407, Aug. 1965, pp. 559-572.

6. Ffowcs Williams, J. E.; and Hawkings, D. L.: Sound Generation by Turbulence and Surfaces in Arbitrary Motion. Philos. Trans. R. Soc. London, ser. A, vol. 264, no. 1151, May 8, 1969, pp. 321-342.

7. Farassat, F.: Theory of Noise Generation From Moving Bodies With an Application to Helicopter Rotors. NASA TR R-451, 1975.

8. Conte, S. D.; and de Boor, Carl: Elementary Numerical Analysis. Second ed. McGraw-Hill Book Co., c.1972.

9. Mixson, John S.; Barton, C. Kearney; Piersol, Alan G.; and Wilby, John F.: Characteristics of Propeller Noise on an Aircraft Fuselage Related to Interior Noise Transmission. AIAA Paper 79-0646, Mar. 1979.

10. Brooks, Bennett M.; and Metzger, F. B.: Acoustic Test and Analysis of Three Advanced Turboprop Models. NASA CR-159667, 1980.

11. Amiet, Roy K.: Correction of Open Jet Wind Tunnel Measurements for Shear Layer Refraction. AIAA Paper 75-532, Mar. 1975.

12. Hanson, Donald B.: The Influence of Propeller Design Parameters on Far Field Harmonic Noise in Forward Flight. AIAA Paper 79-0609, Mar. 1979.

13. Yu, Yung H.; Caradonna, Frank X.; and Schmitz, Fredric H.: The Influence of the Transonic Flow Field on High-Speed Helicopter Impulsive Noise. Paper No. 58, U.S. Army Res. & Technol. Lab. (AVRADCOM) paper presented at Fourth European Rotorcraft and Powered Lift Aircraft Forum (Stresa, Italy), Sept. 1978.

14. Hanson, D. B.; and Fink, M. R.: The Importance of Quadrupole Sources in Prediction of Transonic Tip Speed Propeller Noise. J. Sound & Vib., vol. 62, no. 1, Jan. 8, 1979, pp. 19-38.

15. Hanson, Donald B.: The Aeroacoustics of Advanced Turbopropellers. Paper presented at International Symposium on the Mechanics of Sound Generation in Flows (Göttingen, Germany), Aug. 1979.

TABLE 1.- OPERATING CONDITIONS AND SOME BLADE DATA FOR SR-1 AND SR-3 BLADE DESIGNS

Blade data/operating condition	SR-1	SR-3
Blade radius, m	0.311	0.324
Number of blades	2	4
Rotational speed, rpm	10 040	11 250
Flight Mach number	0.32	0.32
Helical tip Mach number	1.04	1.17
Ambient temperature, ^{o}C	1.7	13.3
Ambient pressure, kPa	92.5	94.6
Blade angle at $(\eta_2/R)_{ref}$ = 0.776, deg	25.7	25.2

TABLE 2.- CORRECTED MICROPHONE POSITIONS FOR ANECHOIC WIND TUNNEL TESTS OF SR-1 AND SR-3 BLADES

[x = distance forward of pitch change axis;
y = distance from propeller axis]

Microphone	x, m	y, m
1	0.351	0.808
2	.162	.808
3	.040	.808
4	-.091	.808
5	-.247	.808
6	-.411	.808
7	-.753	.808

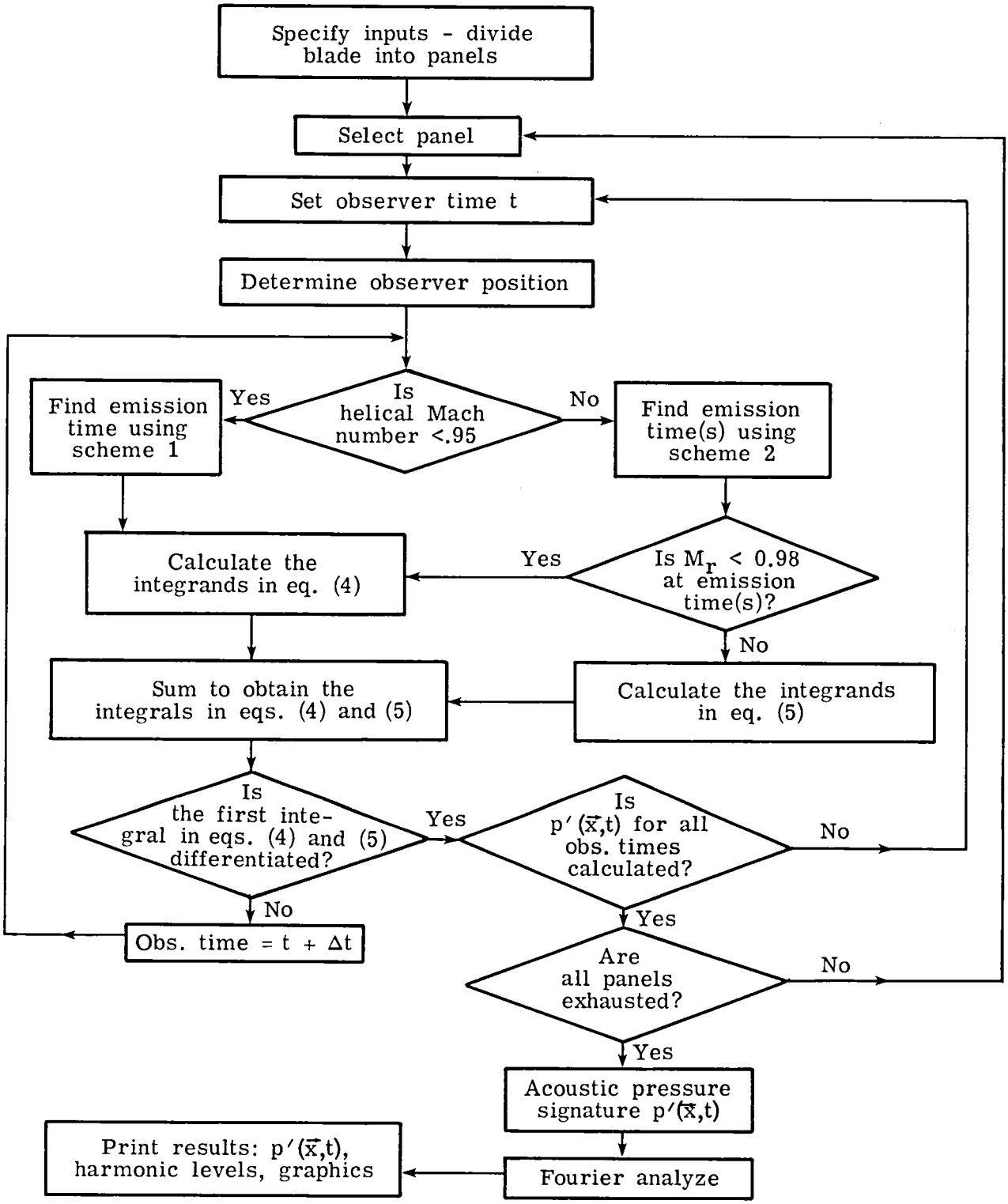

Figure 1.- Flow chart for Langley Acoustic Program.

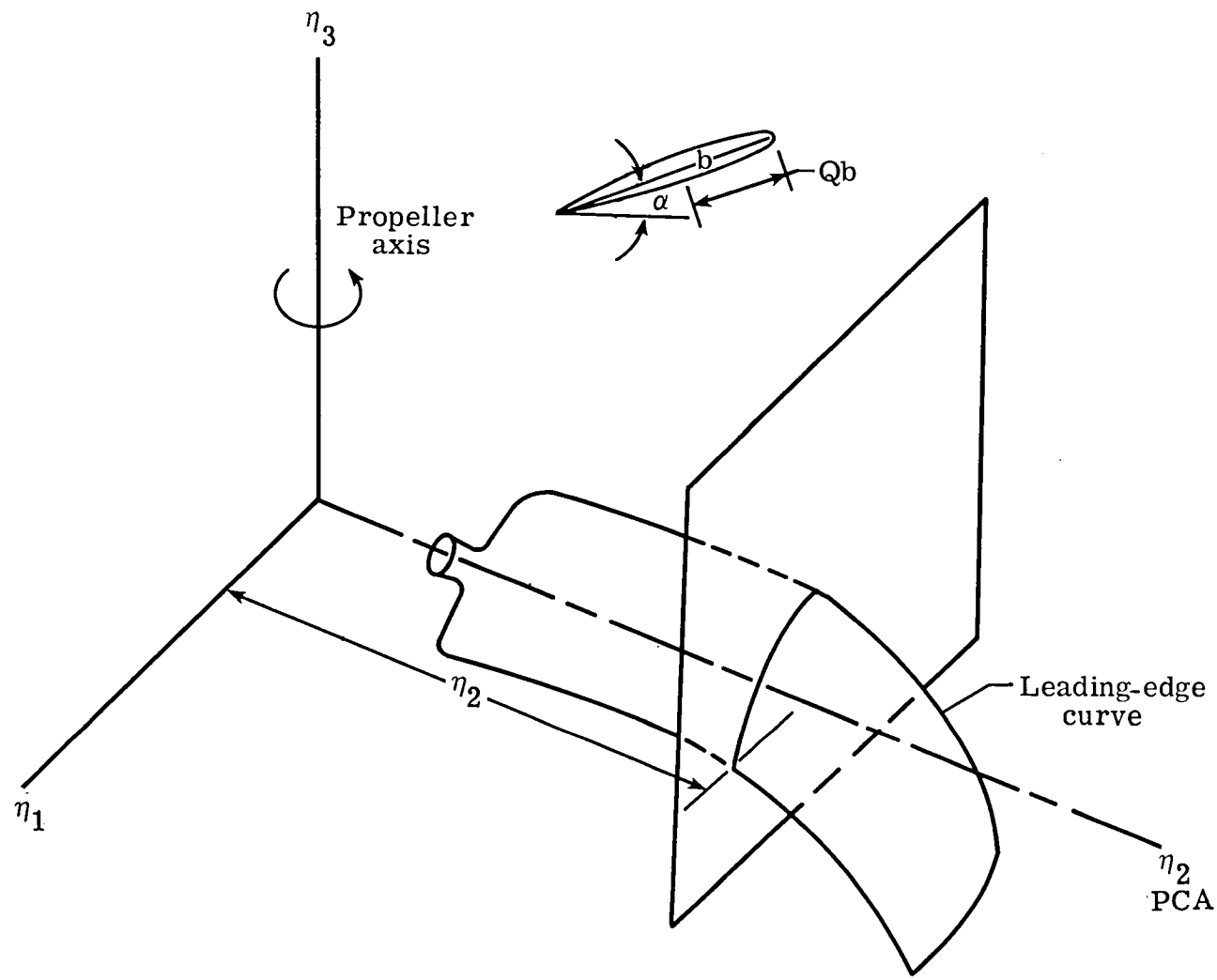

α = geometric angle of attack (function of η_2)

PCA = pitch change axis

b = local chord (function of η_2)

Q = distance from L.E./b

Figure 2.- Curvilinear coordinate system (Q,η_2) used to describe blade geometry of advanced propellers. Blade mean surface is not in a plane.

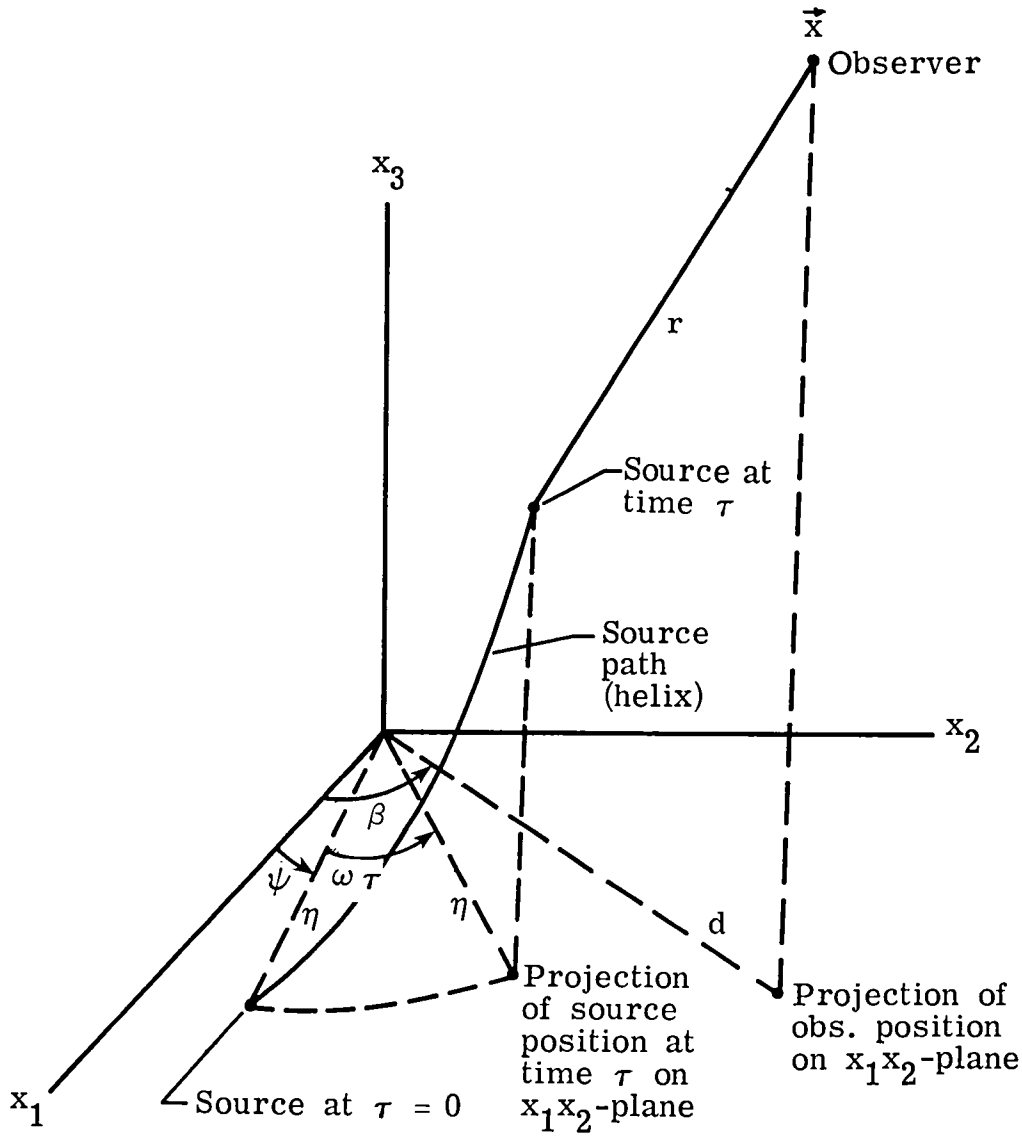

Figure 3.- Geometry of source and observer position used for calculation of emission time in scheme 2. $\phi = \omega\tau + \psi$.

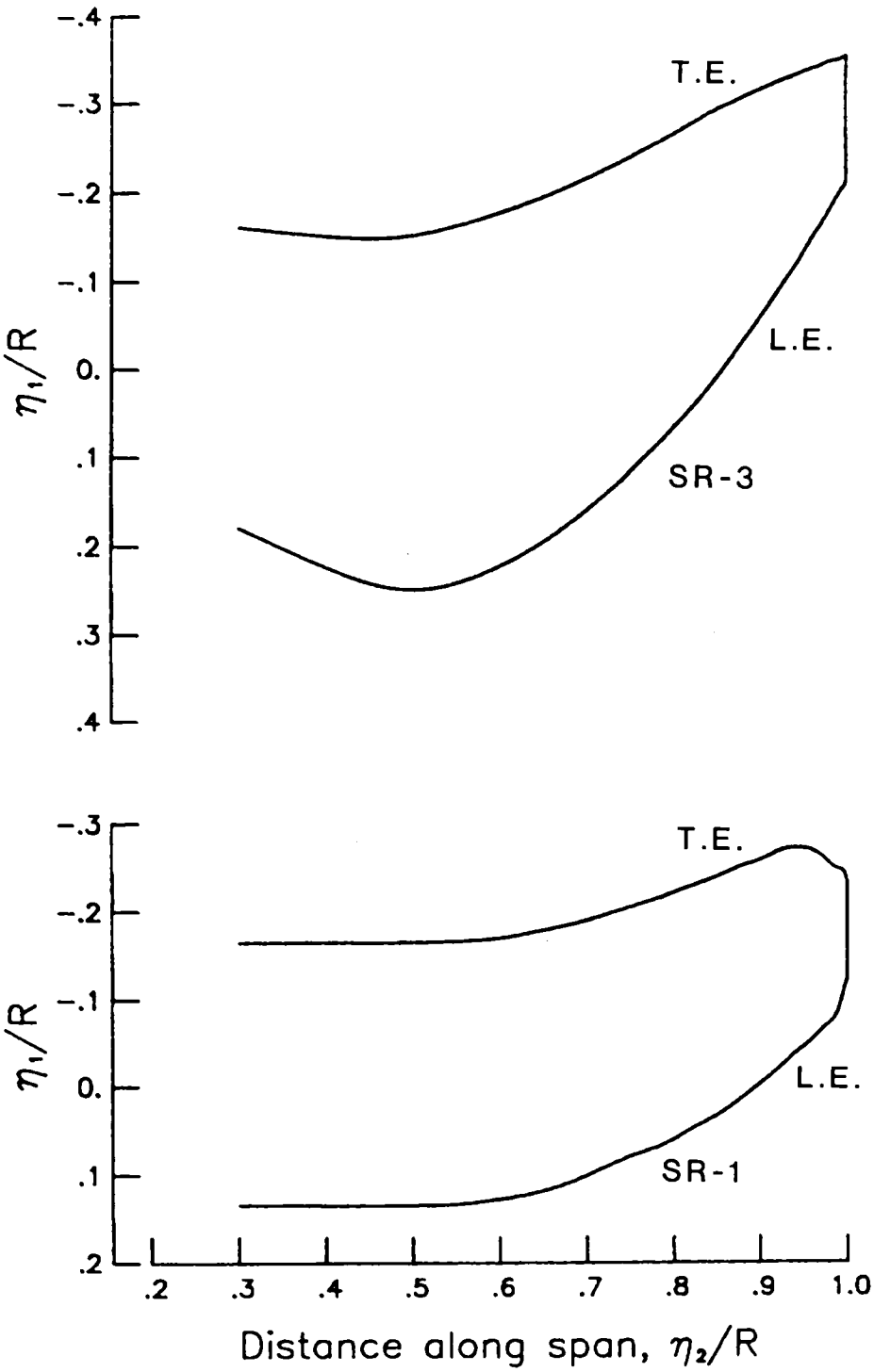

Figure 4.- Planforms of SR-1 and SR-3 blade designs.

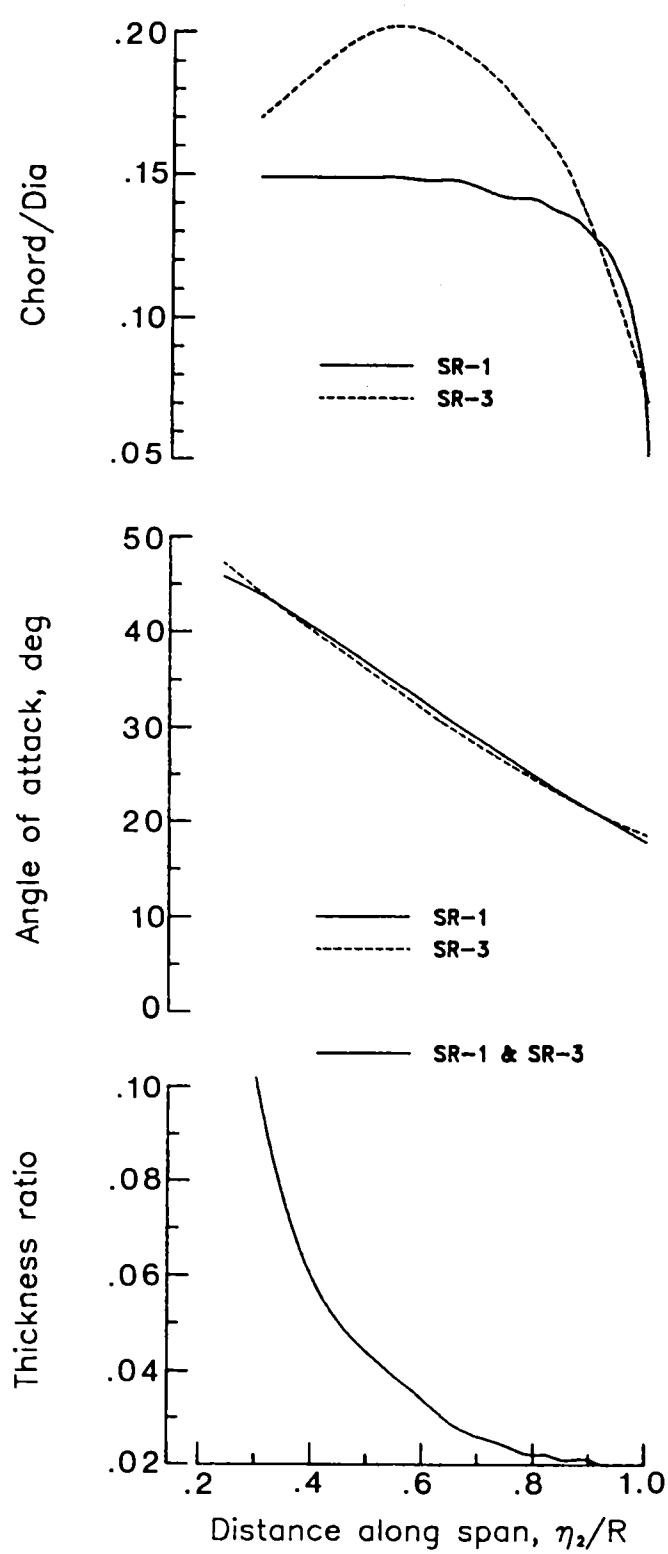

Figure 5.- Blade form curves for SR-1 and SR-3 blade designs.

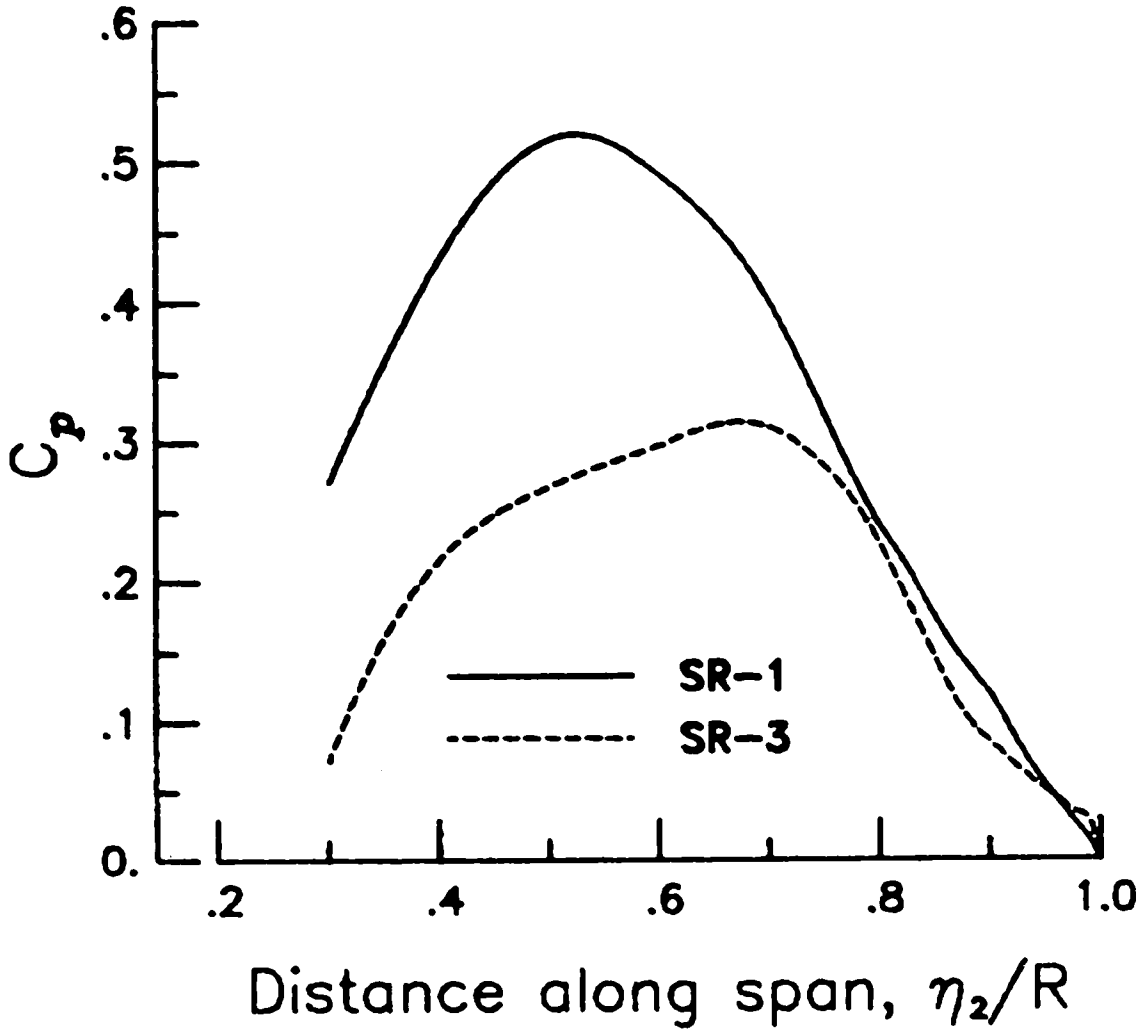

Figure 6.- Theoretical radial distributions of lift coefficients for SR-1 and SR-3 blade designs.

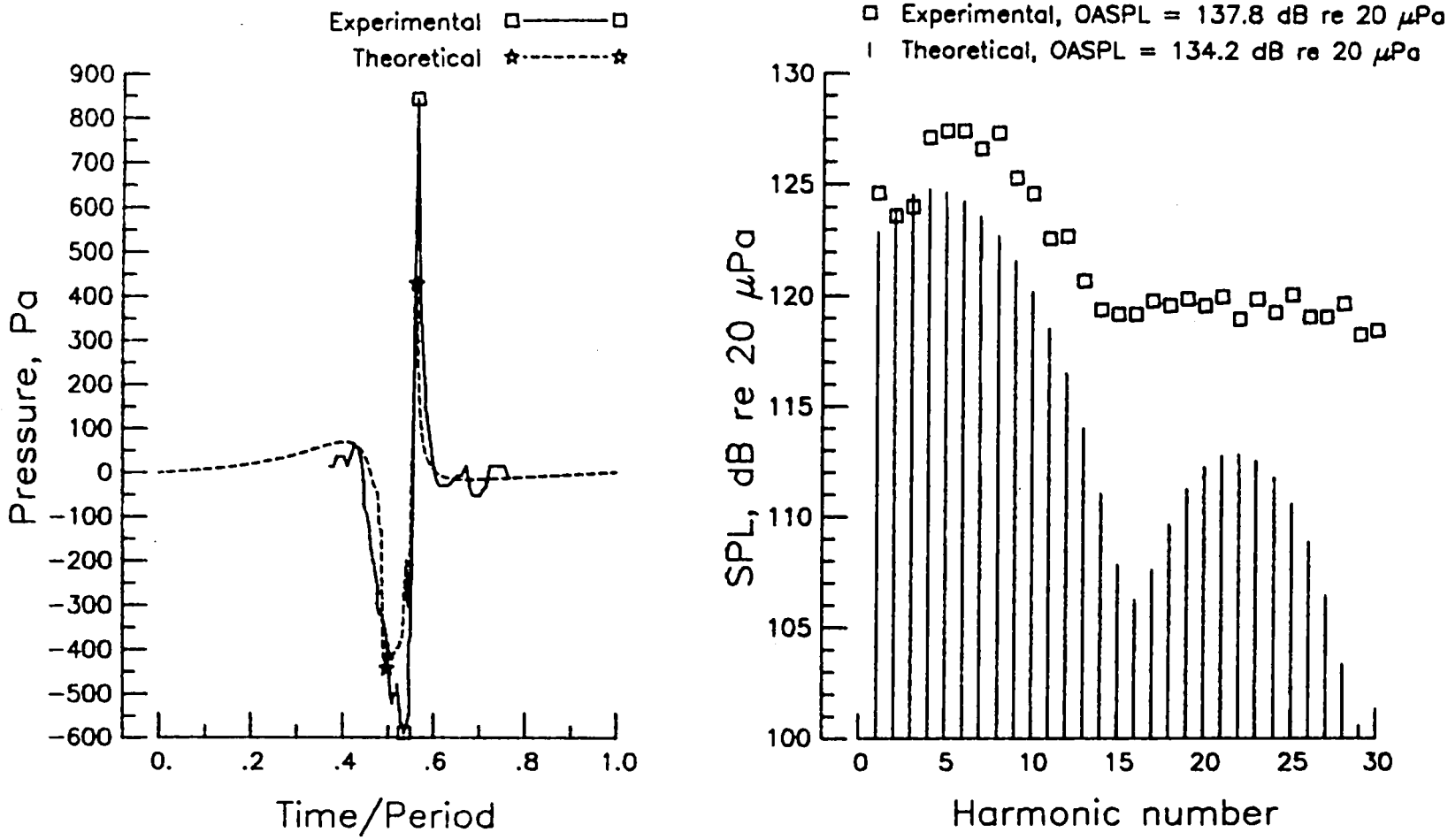

Figure 7.- Comparison of experimental data and theoretical calculations for SR-1 blade, microphone 2.

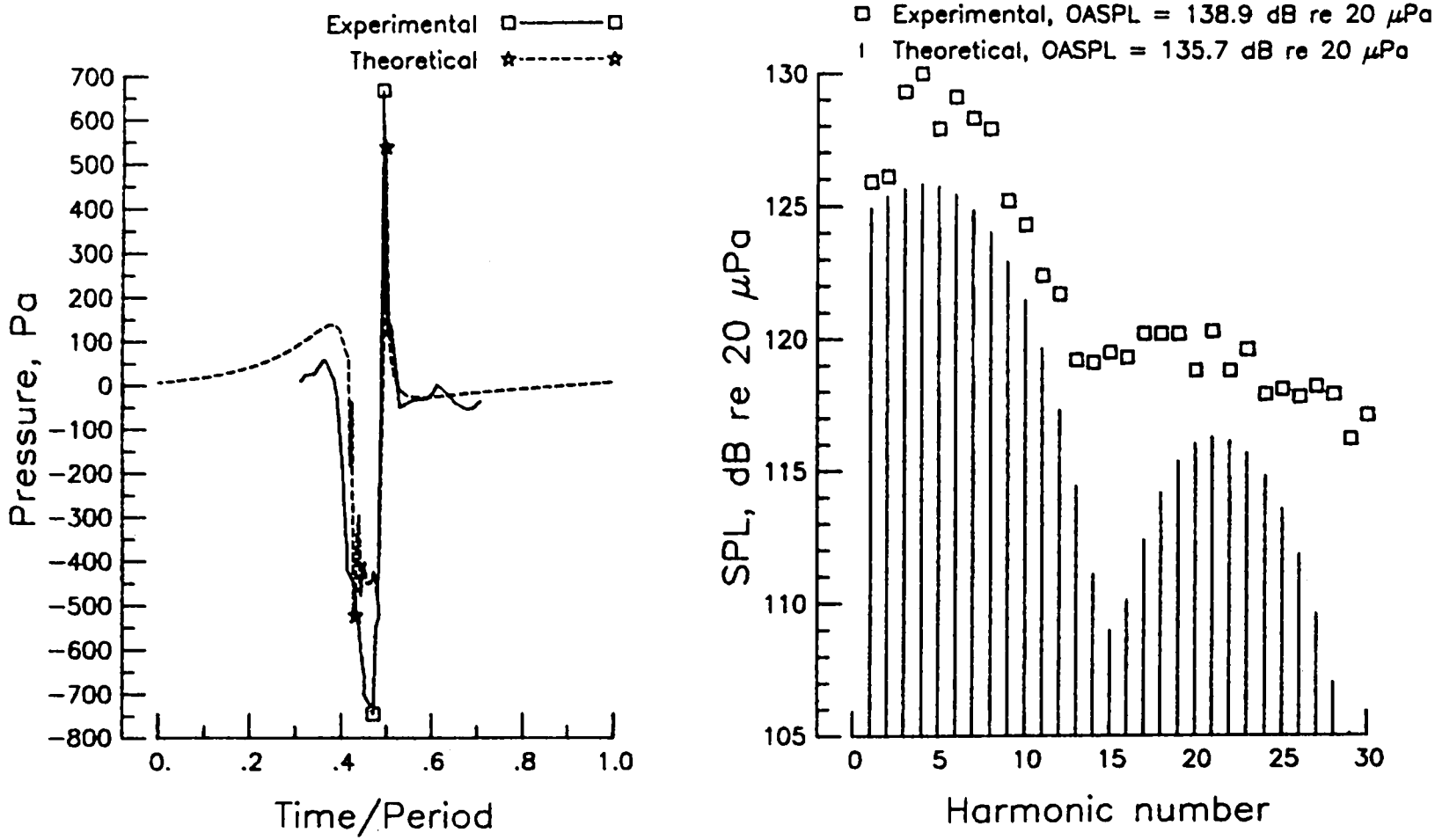

Figure 8.- Comparison of experimental data and theoretical calculations for SR-1 blade, microphone 3.

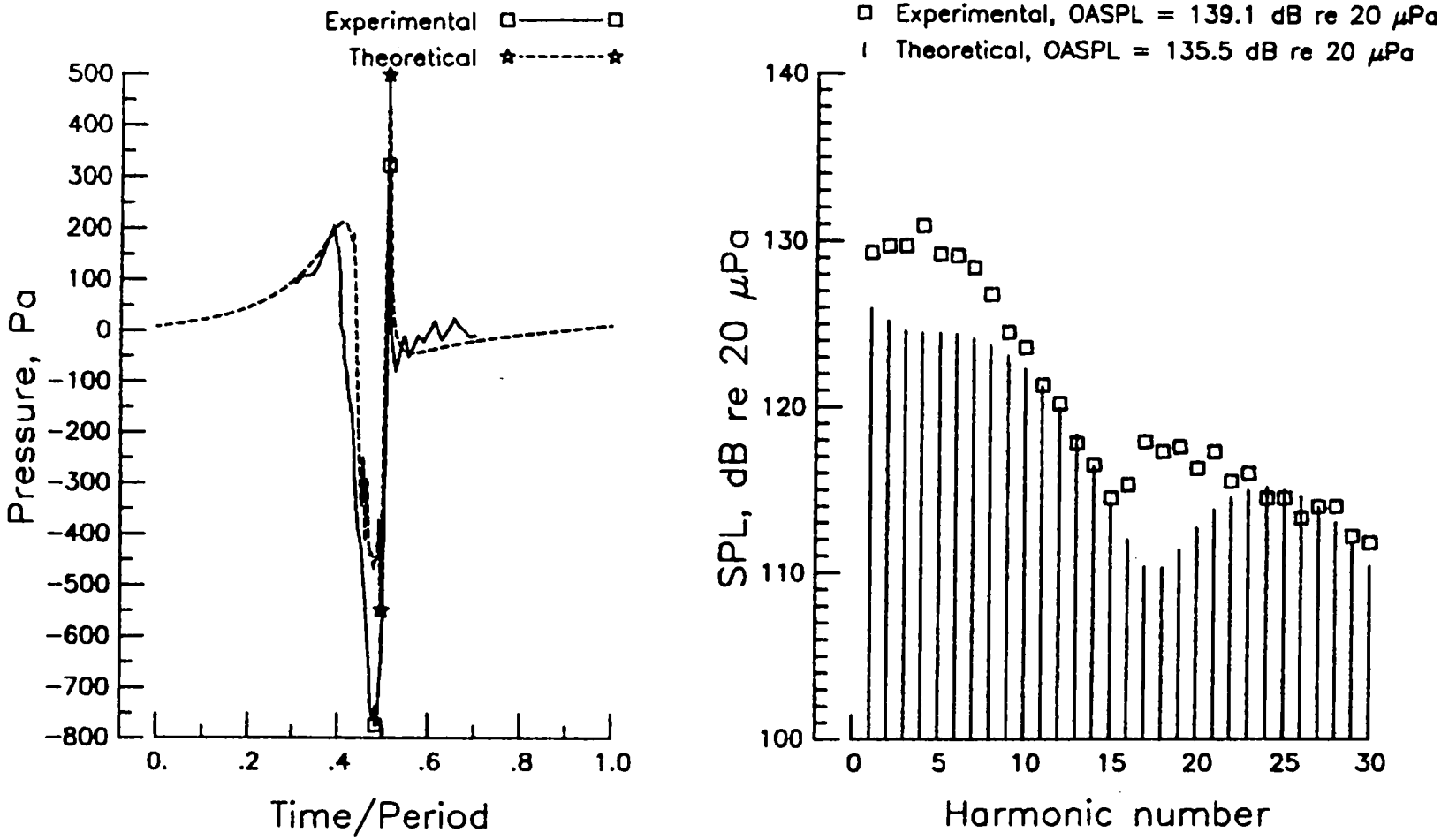

Figure 9.- Comparison of experimental data and theoretical calculations for SR-1 blade, microphone 4.

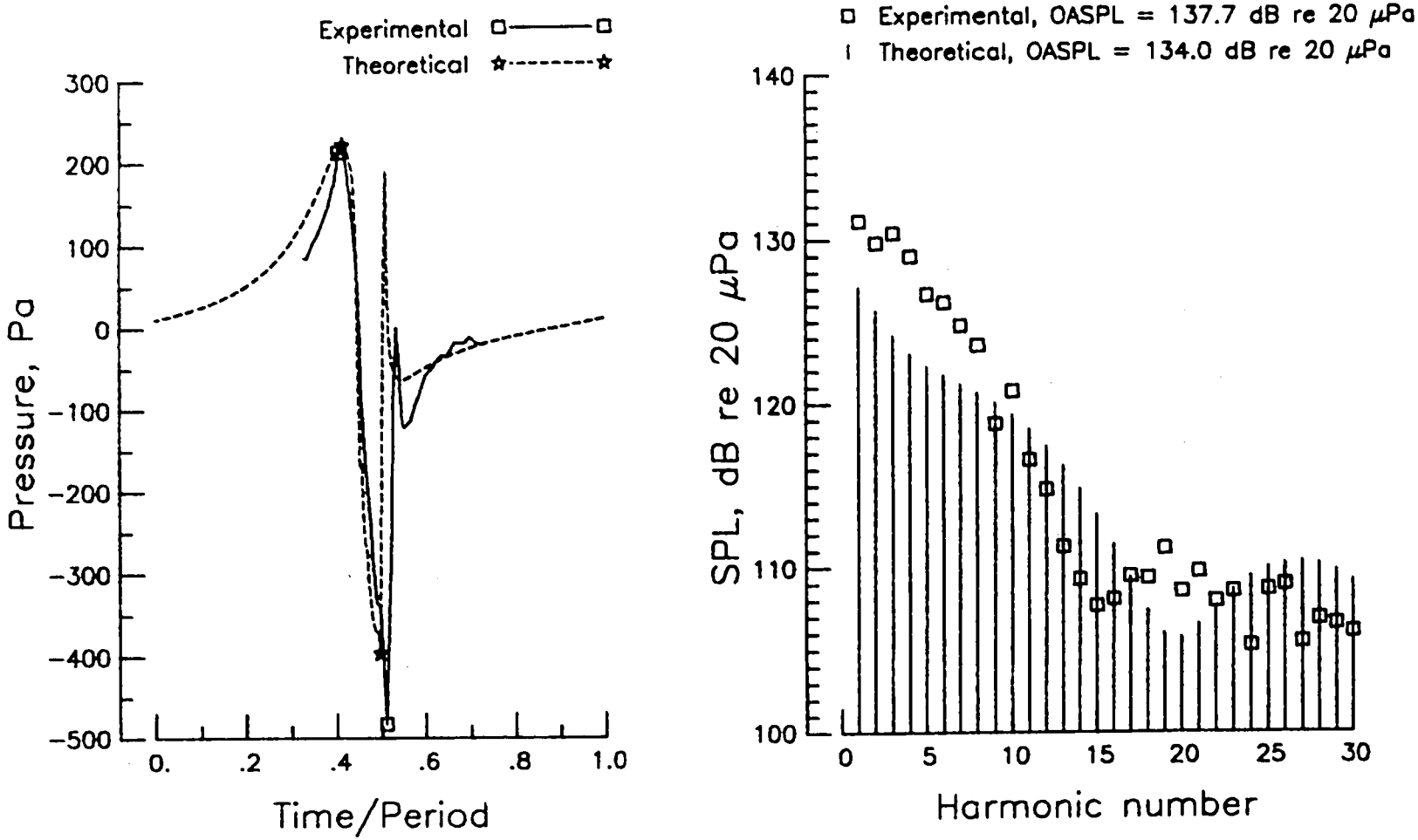

Figure 10.- Comparison of experimental data and theoretical calculations for SR-1 blade, microphone 5.

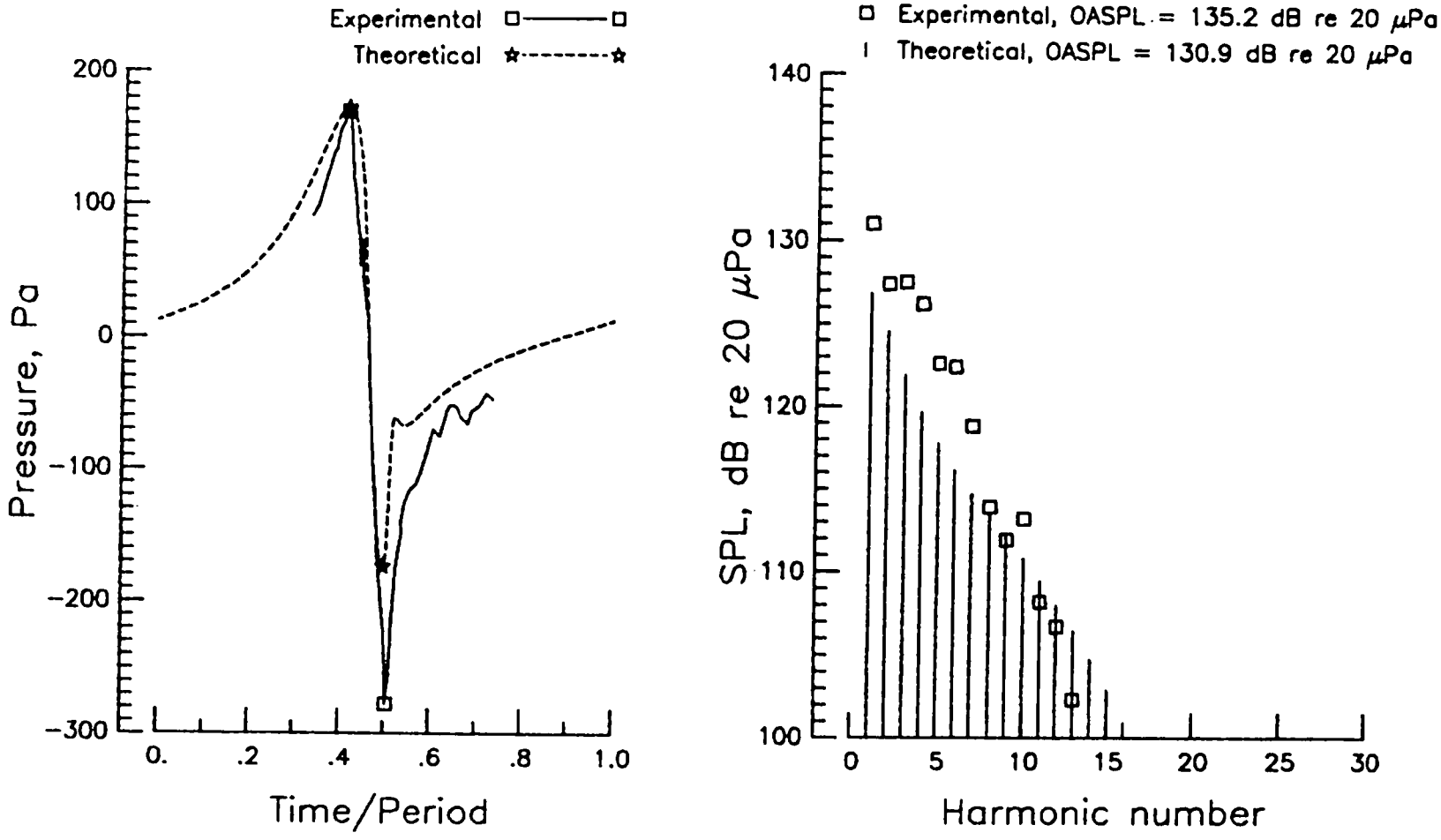

Figure 11.- Comparison of experimental data and theoretical calculations for SR-1 blade, microphone 6.

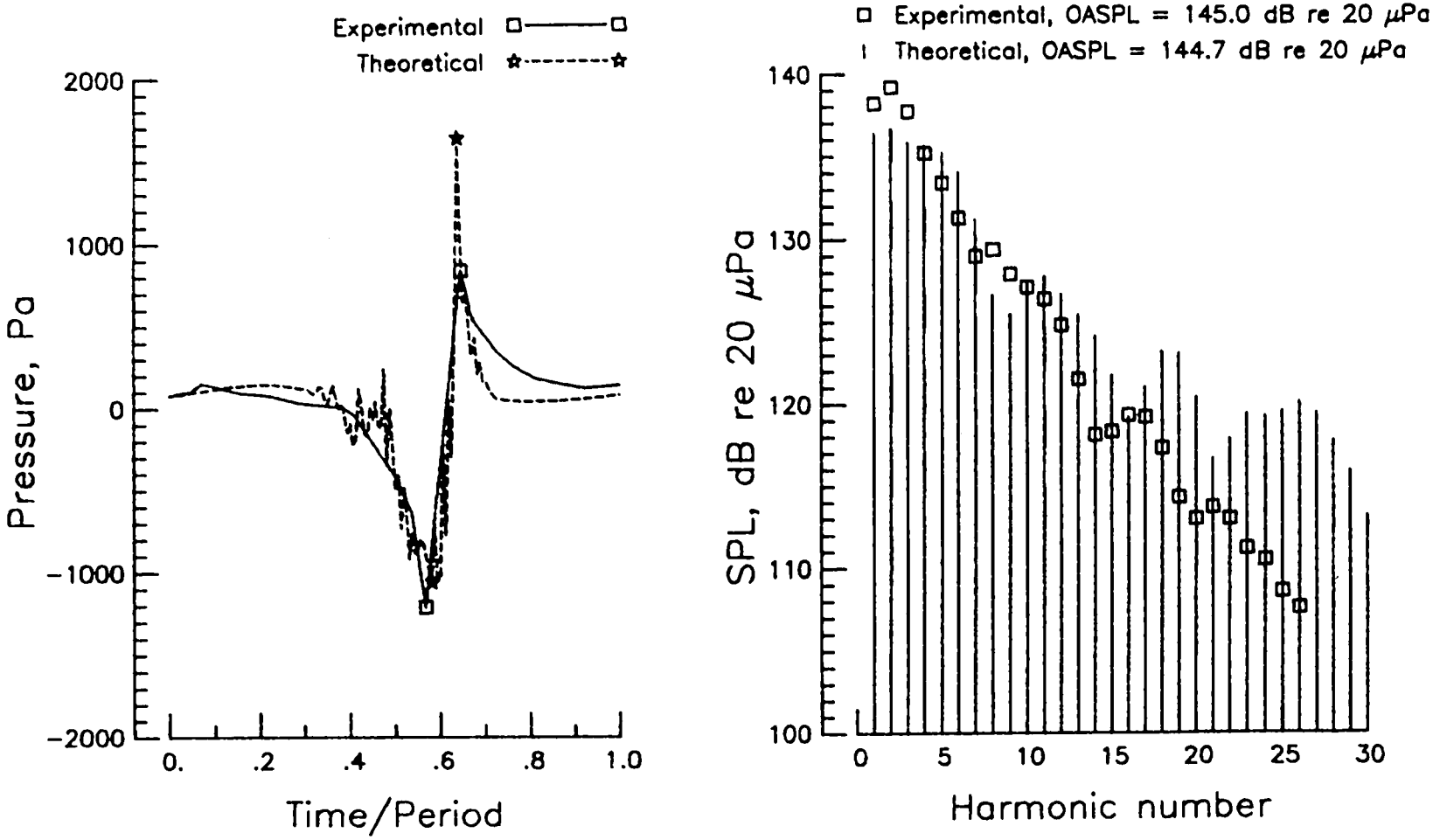

Figure 12.- Comparison of experimental data and theoretical calculations for SR-3 blade, microphone 3.

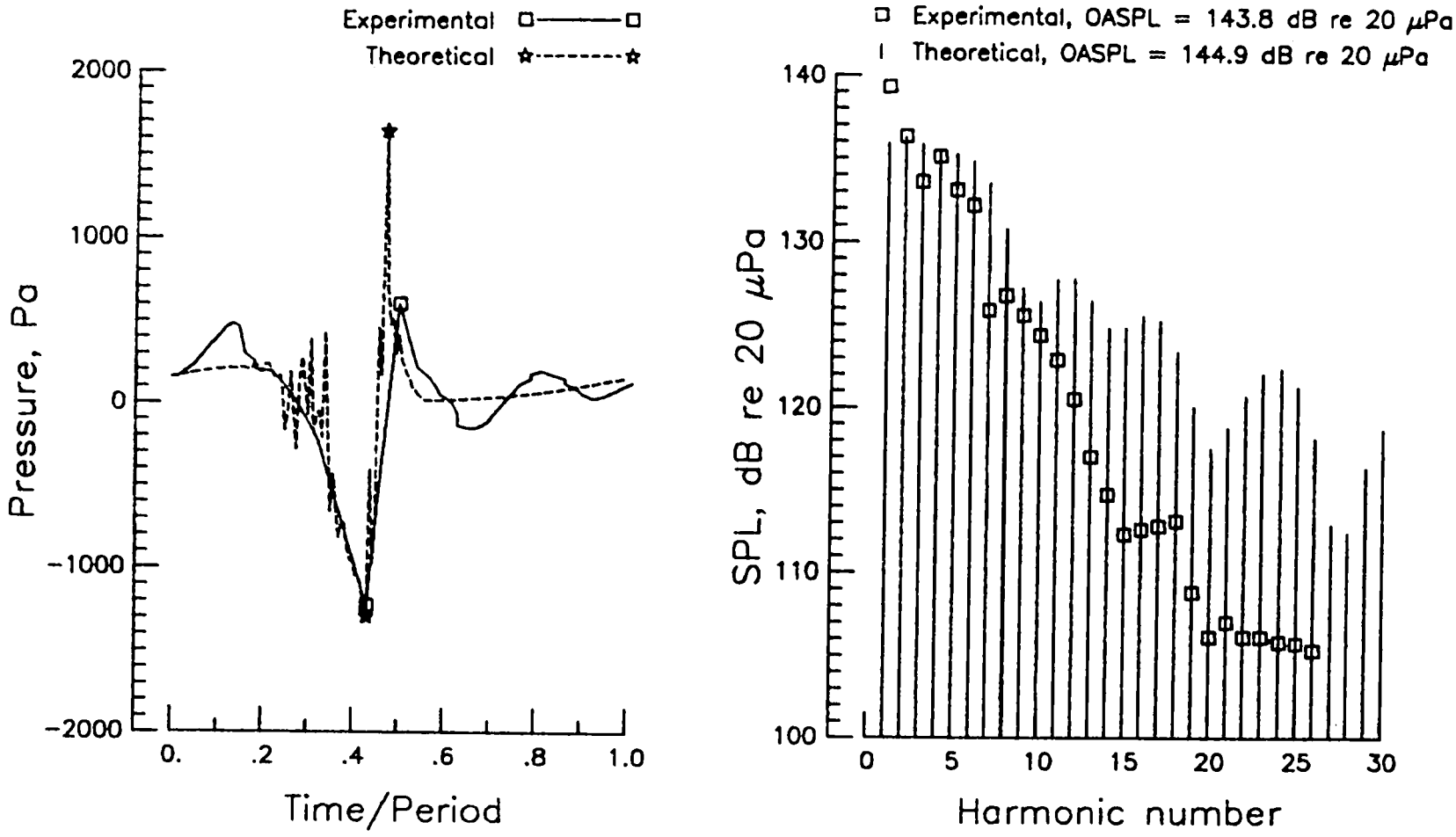

Figure 13.- Comparison of experimental data and theoretical calculations for SR-3 blade, microphone 4.

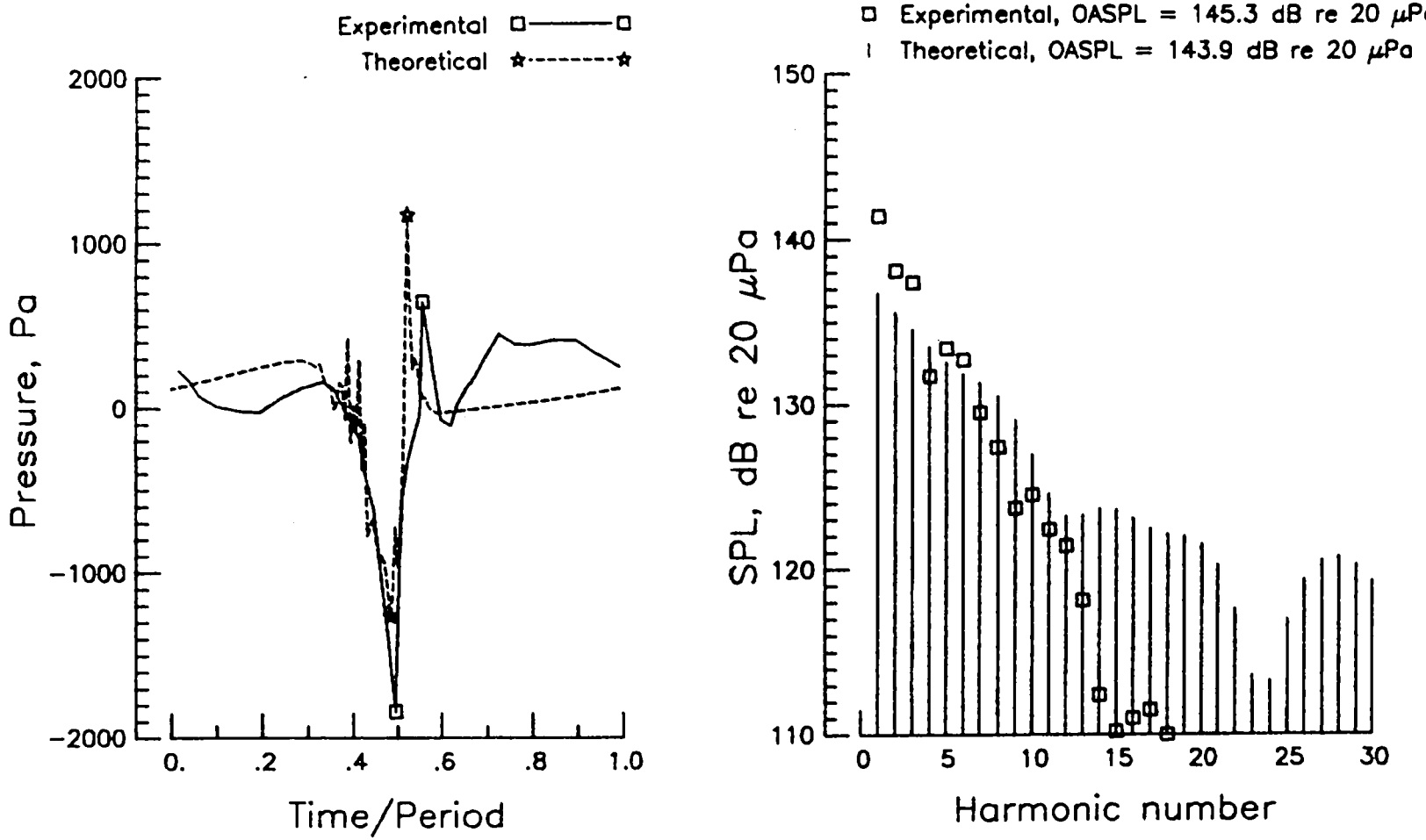

Figure 14.- Comparison of experimental data and theoretical calculations for SR-3 blade, microphone 5.

1. Report No.	2. Government Accession No.	3. Recipient's Catalog No.
NASA TP-1662		

4. Title and Subtitle	5. Report Date
A NUMERICAL TECHNIQUE FOR CALCULATION OF THE NOISE OF HIGH-SPEED PROPELLERS WITH ADVANCED BLADE GEOMETRY	July 1980
	6. Performing Organization Code
7. Author(s)	8. Performing Organization Report No.
Paul A. Nystrom and F. Farassat	L-13535
	10. Work Unit No.
9. Performing Organization Name and Address	505-42-13-05
NASA Langley Research Center Hampton, VA 23665	11. Contract or Grant No.
	13. Type of Report and Period Covered
12. Sponsoring Agency Name and Address	Technical Paper
National Aeronautics and Space Administration Washington, DC 20546	14. Sponsoring Agency Code

15. Supplementary Notes

16. Abstract

This paper discusses a numerical technique and a computer program developed for the prediction of the noise of propellers with advanced geometry. The blade upper and lower surfaces are described by a curvilinear coordinate system, which is also used to divide the blade surfaces into panels. Two different acoustic formulations in the time domain are used to improve the speed and efficiency of the noise calculations: an acoustic formulation with the Doppler factor singularity for panels moving at subsonic speeds and the collapsing sphere formulation for panels moving at transonic or supersonic speeds. This second formulation involves a sphere which is centered at the observer position and whose radius decreases at the speed of sound. The acoustic equation consists of integrals over the curve of intersection for both the sphere and the panels on the blade. Algorithms used in some parts of the computer program are discussed briefly. Some comparisons with measured acoustic data for two model high-speed propellers with advanced geometry are also presented.

17. Key Words (Suggested by Author(s))	18. Distribution Statement
Noise Prediction Propeller Supersonic	Unclassified - Unlimited Subject Category 71

19. Security Classif. (of this report)	20. Security Classif. (of this page)	21. No. of Pages	22. Price*
Unclassified	Unclassified	30	A03

For sale by the National Technical Information Service, Springfield, Virginia 22161

NASA-Langley, 1980

National Aeronautics and
Space Administration

Washington, D.C.
20546

Official Business
Penalty for Private Use, $300

THIRD-CLASS BULK RATE

Postage and Fees Paid
National Aeronautics and
Space Administration
NASA-451

U.S.MAIL

NASA

If Undeliverable (Section 158
Postal Manual) Do Not Return

DO NOT REMOVE SLIP FROM MATERIAL

Delete your name from this slip when returning material to the library.

NAME	DATE	MS
~~John Preisser~~	~~1/30/95~~	~~410~~
Le Trang Nguyen	8/11/95	904

NASA Langley (Rev. Dec. 1991) RIAD N-75